

# Stretchable and Waterproof Self-Charging Power System for Harvesting Energy from Diverse Deformation and Powering Wearable Electronics

Fang Yi,<sup>†,‡,#</sup> Jie Wang,<sup>†,§,#</sup> Xiaofeng Wang,<sup>†,||,#</sup> Simiao Niu,<sup>†</sup> Shengming Li,<sup>†</sup> Qingliang Liao,<sup>‡</sup> Youlong Xu,<sup>§</sup> Zheng You,<sup>||</sup> Yue Zhang,<sup>\*,‡</sup> and Zhong Lin Wang<sup>\*,†,⊥</sup>

<sup>†</sup>School of Materials Science and Engineering, Georgia Institute of Technology, Atlanta, Georgia 30332-0245, United States

<sup>‡</sup>State Key Laboratory for Advanced Metals and Materials, School of Materials Science and Engineering, Beijing Municipal Key Laboratory of New Energy Materials and Technologies, University of Science and Technology Beijing, Beijing 100083, China

<sup>§</sup>Electronic Materials Research Laboratory, Key Laboratory of the Ministry of Education and International Center of Dielectric Research, Xi'an Jiaotong University, Xi'an 710049, China

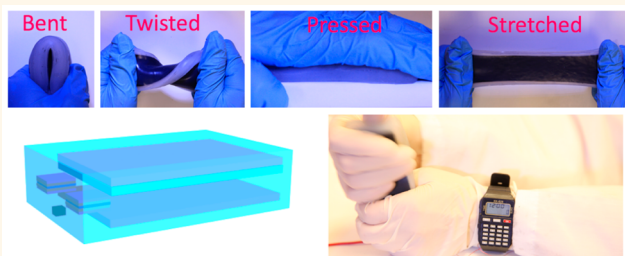
<sup>||</sup>Department of Precision Instrument, Tsinghua University, Beijing 100084, China

<sup>⊥</sup>Beijing Institute of Nanoenergy and Nanosystems, Chinese Academy of Sciences, Beijing, 100083, China

## S Supporting Information

**ABSTRACT:** A soft, stretchable, and fully enclosed self-charging power system is developed by seamlessly combining a stretchable triboelectric nanogenerator with stretchable supercapacitors, which can be subject to and harvest energy from almost all kinds of large-degree deformation due to its fully soft structure. The power system is washable and waterproof owing to its fully enclosed structure and hydrophobic property of its exterior surface. The power system can be worn on the human body to effectively scavenge energy from various kinds of human motion, and it is demonstrated that the wearable power source is able to drive an electronic watch. This work provides a feasible approach to design stretchable, wearable power sources and electronics.

**KEYWORDS:** self-charging, stretchable, wearable, triboelectric nanogenerator, supercapacitor



Stretchable and wearable electronics have been an emerging class of electronics that enable a wide range of applications such as electronic skins, implantable devices, robotics, and prosthetics.<sup>1–5</sup> Consequently, the development of stretchable power sources for such devices is highly demanded with the possibility that they can harvest energy from the environment in which the device is deployed. The triboelectric nanogenerator (TENG) is an attractive renewable power source due to its advantages of low cost, light weight, high efficiency, and eco-friendly feature.<sup>6–16</sup> However, the electrical outputs generated by a TENG are pulses and sometimes with irregular magnitudes owing to the uneven strength of the mechanical motion. To enable it to serve as a direct power source for most electronic devices that need a constant direct-current supply, it is necessary to integrate the TENG with an energy storage device. For this purpose, a supercapacitor (SC) is a choice because of its high power and energy density, cycle efficiency, and charging/

discharging rates compared with batteries and conventional dielectric capacitors.<sup>17–21</sup> Therefore, a stretchable self-charging power system combining a stretchable TENG and stretchable SCs is a promising solution. Up to now, the self-charging power systems that have been reported focus on converting ambient energy to a direct power source, but they were not stretchable, which cannot satisfy the need for stretchable electronics.<sup>22–26</sup> Recently, there have been studies about stretchable TENGs based on stretchable or wavy-structured polymers and stretchable SCs based on conductive buckled structures or fiber springs.<sup>27–33</sup> Still, further research is highly required to extend the stretchability, optimize the device structure, improve the performance, and subsequently create a proper integration of the two parts. In addition, a self-protection from the external

Received: May 6, 2016

Accepted: June 22, 2016

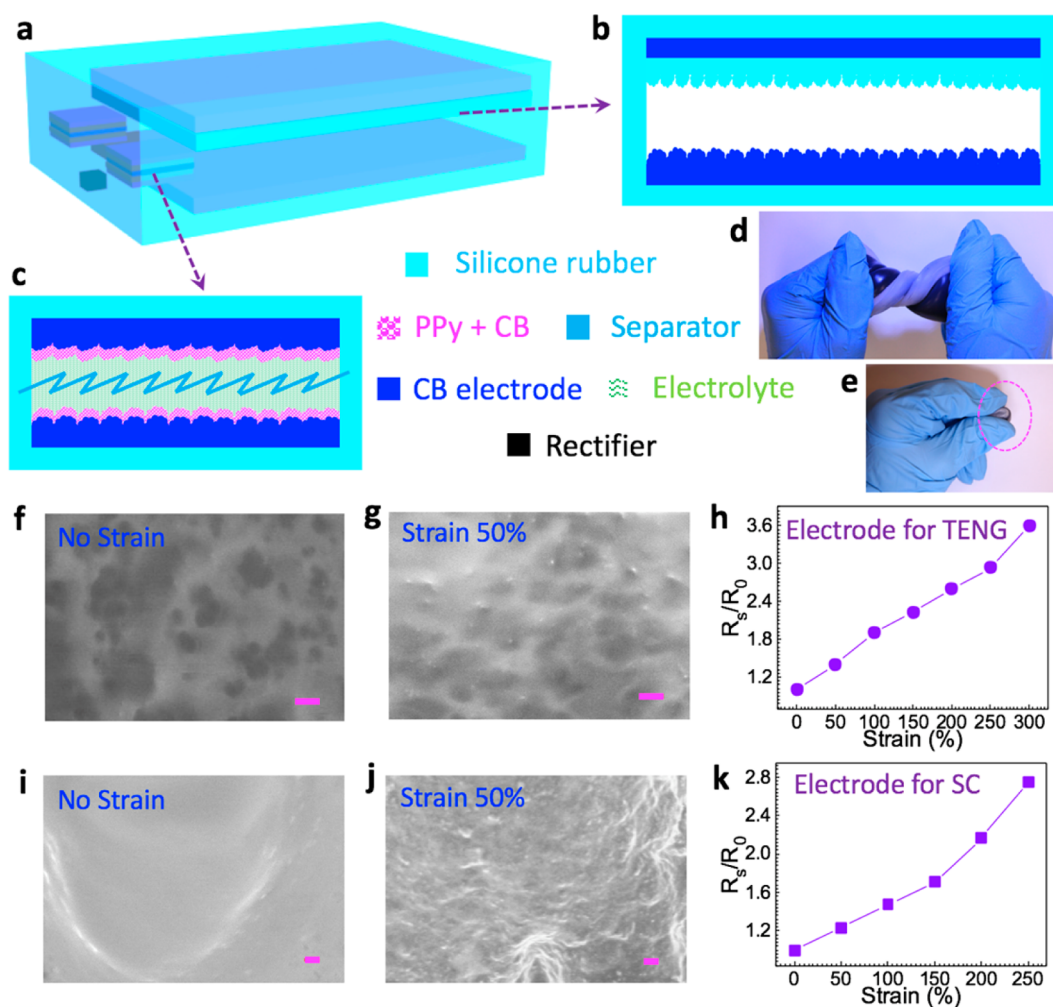


**Figure 1.** Structure design of a stretchable, fully enclosed self-charging power system. (a–c) Schematic diagram showing the detailed structure of the power system: (a) perspective view of the power system; (b) cross-sectional view of the TENG part; (c) cross-sectional view of the SC part. (d) Photograph showing the power system in the twisted state. (e) Photograph showing the SC in the bent state. (f, g) SEM images of the surface morphology of the TENG's electrode (f) in the original state and (g) in the stretched state. Scale bar: 1  $\mu\text{m}$ . (h) Relationship between the resistance of the TENG's electrode and the tensile strain. (i, j) SEM images of the surface morphology of the SC's electrode (i) in the original state and (j) in the stretched state. Scale bar: 1  $\mu\text{m}$ . (k) Relationship between the resistance of the SC's electrode and the tensile strain.

environment is preferable for stretchable power sources so as to adapt to real-world conditions.

Here, we introduce a kind of self-charging power system that can not only be bent but also be stretched, compressed, twisted, and deformed into complex, curvilinear shapes, and all such deformation can be converted into electricity. The stretchable self-charging power system (SSCPS) seamlessly integrated a stretchable TENG and stretchable SCs, with the TENG part converting diverse motion into electricity and the SC part storing the harvested energy. The SC was fabricated based on two intrinsically stretchable electrodes, while the TENG and the whole SSCPS were constructed through casting liquid silicone rubber into molds. The SSCPS was washable and waterproof due to its fully enclosed structure and the hydrophobic property of its external surface. The SSCPS was applied to effectively collect energy from various human motions and serve as a direct power source to drive an electronic watch.

## RESULTS AND DISCUSSION

The structure of the SSCPS is schematically depicted in Figure 1a–c, which seamlessly integrates a TENG and two SCs in series. The two triboelectric parts of the stretchable TENG include a layer of stretchable electrode (70 mm  $\times$  38 mm  $\times$  200  $\mu\text{m}$ ) and a layer of silicone rubber (thickness: 200  $\mu\text{m}$ ) with the corresponding stretchable electrode on the top (Figure 1b). There is an air gap ( $\sim$ 1 cm) between the two triboelectric parts to realize the contact and separation of the two parts and thereby the generation of the electrical outputs. The stretchable electrode (resistivity:  $\sim$ 0.30  $\Omega \times \text{m}$ ) of the TENG is a compound of carbon black (CB) and silicone rubber, which will be called a CB electrode in the following. To enhance the triboelectric charge density of the two triboelectric surfaces and increase the contact area between the two triboelectric parts,<sup>34,35</sup> nano/microstructures were created on the surfaces of the two triboelectric parts by using sandpaper. As exhibited in Figure 1c, the stretchable SC (5 mm  $\times$  5 mm) consists of two stretchable electrodes and a wrinkled separator (polyethylene), with poly(vinyl alcohol) (PVA)/phosphoric acid

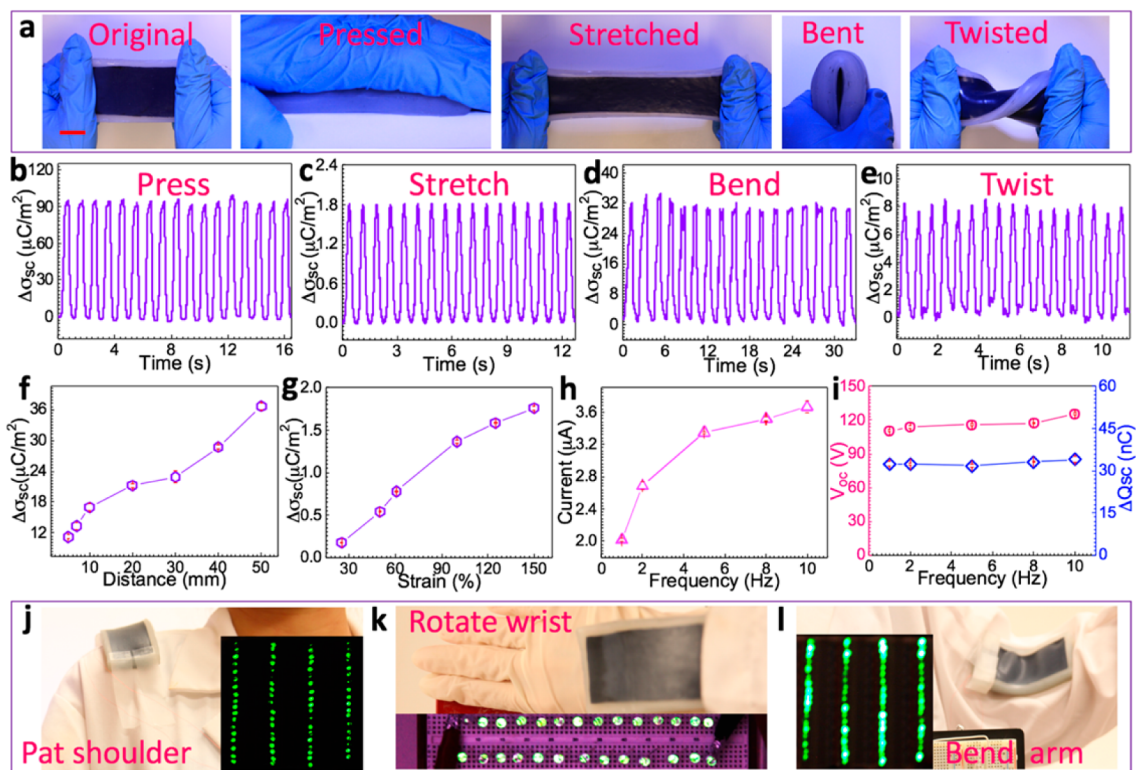


**Figure 2.** Individual performance of the TENG part under various deformations. (a) Photographs showing the device under various deformations. Scale bar: 20 mm. (b–e) Short-circuit transferred charge density ( $\Delta\sigma_{sc}$ ) of the TENG part when the device is under (b) pressing, (c) stretching, (d) bending, and (e) twisting motion. (f) Dependence of the  $\Delta\sigma_{sc}$  on the distance between the contacting object and the device under pressing motion. (g) Summarized relationship between the  $\Delta\sigma_{sc}$  and the elongation of the device. (h) Dependence of the short-circuit current on the frequency. (i) Dependence of the open-circuit voltage ( $V_{oc}$ ) and short-circuit transferred charge on the frequency. (j–l) Demonstration of the TENG part harvesting energy from (j) patting the shoulder, (k) rotating the wrist, and (l) bending the arm.

( $H_3PO_4$ ) gel as the electrolyte. The stretchable electrode of the SC (resistivity:  $\sim 0.46 \Omega \times m$ ) was fabricated by coating a composite of active material (soluble polypyrrole (PPy)) and conducting additive (CB) on the surface of the CB electrode. A silicone rubber wrapper was utilized to package the SC. The flexible, wrinkled separator prevents short-circuiting between the two stretchable electrodes of the SC. Figure 1d and e show an SSCPS in the twisted state and an SC (10 mm  $\times$  18 mm) in the bent state, respectively. The nano/microstructured surface morphologies of the TENG's and SC's stretchable electrodes in the original state and the stretched state are presented in Figure 1f,g and i,j. Although the resistances of the TENG's and SC's electrode both increase with elongation (Figure 1h,k and Figure S1), this increase is acceptable and will have little negative impact on the system's performance. For the TENG part, its high inherent impedance enables the resistance of its electrode to vary within a wide range with little performance degradation (Note S1); for the SC part, the increasing resistance of the electrode leads to a very small decline in its performance (will discuss in detail later). The integration of the TENG part, SC part, and rectifier was achieved by casting liquid silicone rubber into a mold, where the three parts were combined after the silicone rubber cured. Details of the fabrication processes of the stretchable electrodes, the SC, and the SSCPS can be found in Figure S2 and the Experimental Section.

Due to its excellent flexibility and stretchability, the SSCPC can operate under diverse deformation without any mechanical failure. The individual performance of the TENG part of the SSCPC is presented in Figure 2. By pressing, stretching,

bending, or twisting the device (Figure 2a), electrical outputs were generated. The measured short-circuit charge density ( $\Delta\sigma_{sc}$ ) signals upon such kinds of motion are presented in Figure 2b–e, while the open-circuit voltage ( $V_{oc}$ ) and short-circuit current density are presented in Figure S3. It can be seen that the TENG part can reveal a  $V_{oc}$  of as high as  $\sim 400$  V and a  $\Delta\sigma_{sc}$  of as high as  $\sim 97 \mu C m^{-2}$  by extracting energy from human motion. The TENG part exhibits higher electrical outputs under pressing motion than under other kinds of motion for three reasons. First, there is a much larger relative displacement between the two triboelectric parts under a pressing motion. Second, the two soft triboelectric parts have a much more effective contact area under the pressing motion. Third, under a pressing motion, besides the relative displacement between the two triboelectric parts, the contact/separation between the two triboelectric parts, the contact/separation between the human hand and the device also contributes to the electrical outputs. In Figure 2c,d and Figure S3b,c, the TENG part exhibits higher electrical outputs under bending motion than under stretching motion. This is because for the electrical outputs under bending motion the two triboelectric parts have a larger relative displacement and more effective contact area, whereas for the electrical outputs under stretching motion, the relative displacement is too small to even induce a contact between the two triboelectric parts. The schematic illustration of the working mechanism under diverse deformation is exhibited in Figure S4, which is based on the coupling of the triboelectric effect and electrostatic induction. Since the silicone rubber has a high ability to attract electrons, it will become negatively charged after contacting a material

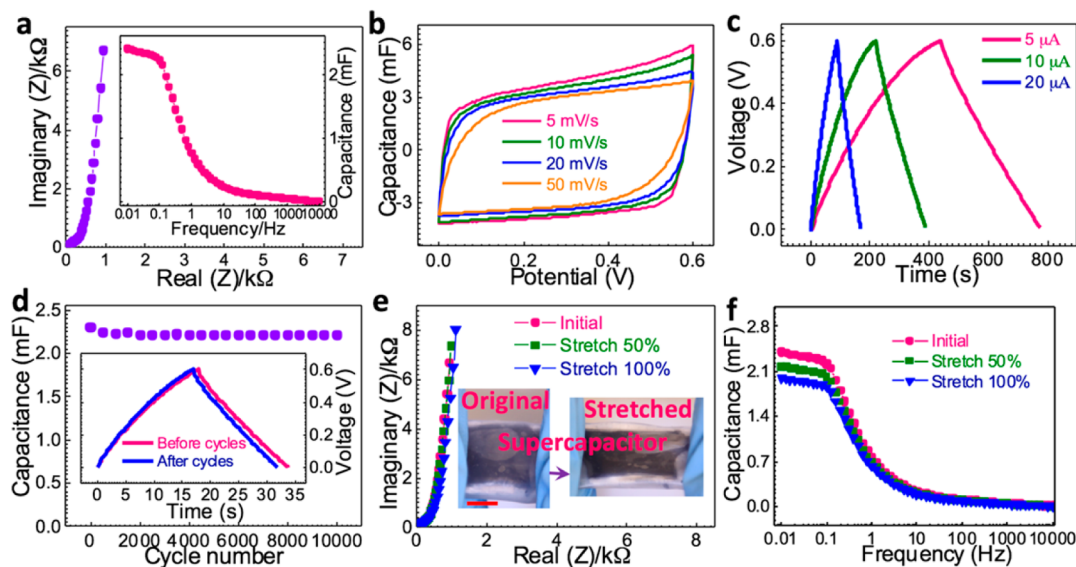


**Figure 3.** Individual performance of the SC. (a) Electrochemical impedance spectroscopy, with the inset showing the capacitance *versus* frequency. (b) Cyclic voltammetry curves of the SC at different scanning rates. (c) Galvanostatic charging/discharging profiles at different current densities of the SC. (d) Stability test of the SC, with the inset showing the charging/discharging curves before and after 10 000 cycles. (e, f) Electrochemical impedance spectroscopy of the SC in the stretched state: (e) imaginary part of the impedance at different frequencies. Scale bar: 5 mm. (f) Capacitance *versus* frequency.

having a lower ability to attract electrons, leaving the material positively charged. The TENG part can work in the attached-electrode mode, the single-electrode mode, and a combination of the two modes. The attached-electrode mode refers to the contact electrification inside the TENG part. The change of the distance between the top silicone rubber and the bottom stretchable electrode due to deformation induces an electrical potential difference between the two electrodes of the TENG in the open-circuit condition, which drives electrons to flow through the external load in the short-circuit condition. The repeated approaching and separation of the two triboelectric parts produces an alternating current. The single-electrode mode refers to the contact electrification between the device and an external object. The approaching and separation between the external object and the outer surface of the device can lead to the electric potential difference between the two electrodes and trigger the charge transfer between the two electrodes. If the external object causes deformation of the device, both working modes will contribute to the electricity generation. When the distance between the object (an acrylic plate was utilized in the experiment) and the device becomes larger under pressing motion, there is an increase of the measured short-circuit transferred charge density ( $\Delta\sigma_{sc}$ ) from  $\sim 11.22 \mu\text{C m}^{-2}$  to  $\sim 36.6 \mu\text{C m}^{-2}$  (Figure 2f) and the  $V_{oc}$  from  $\sim 86.68$  to  $\sim 223.81$  V (Figure S5a). Note that the maximum electrical outputs under pressing motion shown in Figures 2f and S5a are smaller than that in Figures 2b and S3a because the relative displacement between the two triboelectric parts (device deformation) is smaller for the outputs in Figures 2f and S5a than that in Figures 2b and S3a. For the stretching deformation, it has been found that the measured  $\Delta\sigma_{sc}$  (Figure 2g) and  $V_{oc}$  (Figure S5b) increase with increased stretching of the device. This is because the relative displacement between the two triboelectric parts increases with the increasing elongation of the device. When the device is periodically pressed by an acrylic plate driven by a shaker, the generated current of the TENG increases with the increasing frequency

(from  $\sim 2.01 \mu\text{A}$  at 1 Hz to  $\sim 3.66 \mu\text{A}$  at 10 Hz), while the short-circuit transferred charge ( $\sim 32$  nC) and the  $V_{oc}$  ( $\sim 116$  V) remain unchanged. Note that the pressing displacement was kept the same at different frequencies. The device can be mounted on curved and soft parts of the human body, such as the joints and the shoulder. Figure 2j–l and Supporting Movies S1–3 show that the TENG part of the SSCPC can efficiently harvest energy from everyday human motion, such as patting the shoulder, bending the arm, and rotating the wrist.

The performance of the stretchable SC, including ionic conductivities, capacitance, kinetic analysis, and cycle ability, was characterized through electrochemical impedance spectroscopy (EIS), cyclic voltammetry (CV), and galvanostatic cycling (GC). Note that the SC has a highly scalable fabrication process and the size of the tested SCs is 10 mm  $\times$  18 mm. Figure 3a shows the EIS curve at open circuit voltage, and it can be seen that the imaginary part of the impedance at low frequencies is almost vertical to the real part, indicating an ideal capacitive behavior. The capacitance as a function of frequency presents a stable high-capacitance plateau at the low-frequencies area, which is 2.4 mF at 10 mHz, suggesting a fast charging/discharging ability (inset of Figure 3a). The rectangle-like CV curves at scanning rates from 5 to 50 mV/s demonstrate the very fast electrochemical switching ability of the SC (Figure 3b). The GC charging/discharging curves at three currents (5, 10, and 20  $\mu\text{A}$ ) are all close to a straight line (Figure 3c), which further validates the ideal capacitive behavior of the SC. The capacitance is calculated from the discharging curves with values of 2.8 and 2.6 mF obtained at current loads of 5 and 20  $\mu\text{A}$ , respectively. It should be noted that the value of the capacitance calculated from the GC data is slightly higher than that calculated from EIS data, which can be attributed to the redox switch hysteresis. The SC is very stable and reliable in operation. As shown in Figure 3d, the capacitance is maintained after 10 000 cycles, and the GC curves remain almost the same before and after the cycling test, especially in the charging process. The SC is highly stretchable

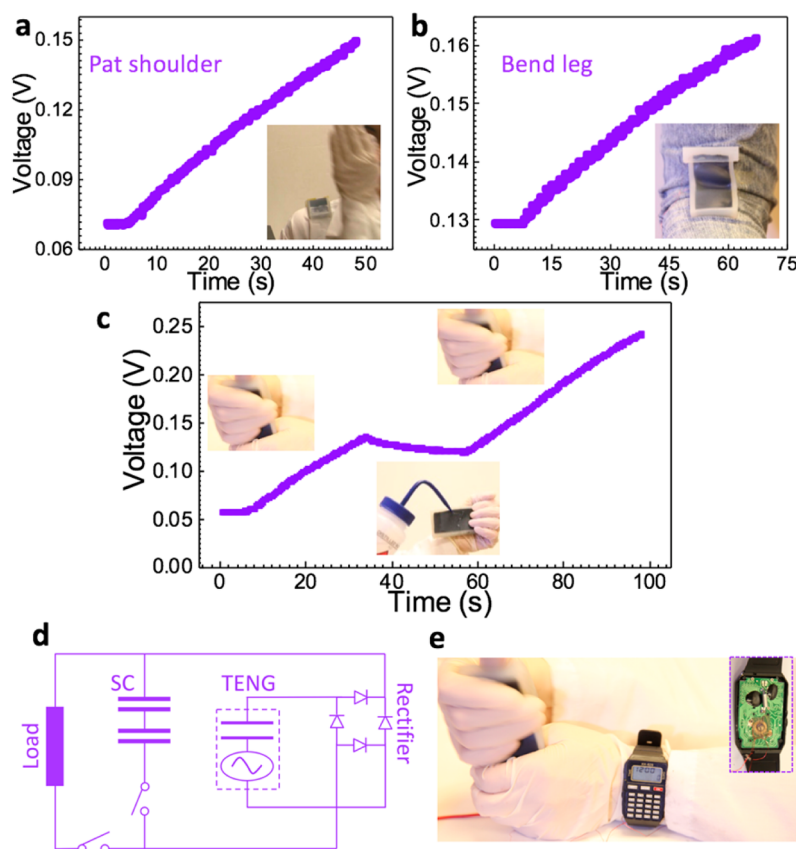


**Figure 4.** Performance of the stretchable self-charging power system. (a) Charging curve of the SC by patting the shoulder. (b) Charging curve of the SC by bending the leg. (c) Charging curve of the SC before and after the power system was washed with water. (d) Circuit diagram of the power system with a load. (e) Photograph showing an electric watch driven by the self-charging power system.

and can endure a strain of 100% while suffering only a small decrease in performance. Figure 3e shows that when the SC is stretched, there is a slight right shift of the imaginary part in the EIS curve at low frequencies, and the capacitance as a function of frequency shows a tiny decrease under stretching (Figure 3f). This can be attributed to the increasing resistance of the SC's electrodes with the stretching (Figure 1k). To create an efficient self-charging process, it is favorable that the supercapacitor has a low leakage current. The low leakage nature of the stretchable SC enables it to be efficiently charged by the TENG.

The self-charging behavior of the SSCPS was realized by connecting the TENG with two SCs in series through a rectifier that was put at the end of the device. Note that the size of the rectifier is much smaller compared with the whole device structure, and the silicone rubber has a very high stretchability (elongation at break is 900%) and a large tolerance for chip-scale unstretched components; therefore, the rectifier has nearly no impact on the stretchability and performance of the SSCPS. Figure 4 demonstrates the self-charging process of the SSCPS through extracting energy from human motion. When the SSCPS is mounted on the human shoulder, the SC of the SSCPS is charged at a rate of  $\sim 104$  mV/min by patting the shoulder with the hand at  $\sim 1.3$  Hz (Figure 4a), indicating an equivalent galvanostatic current of  $\sim 337$  nA (the detailed calculation process can be found in Note S2), and when the SSCPS is laminated on the knee joint, the SC is charged at a rate of  $\sim 31$  mV/min through bending the leg at  $\sim 1.1$  Hz (Figure 4b). Moreover, the fully enclosed structure of the

SSCPC and the hydrophobic property of the silicone rubber enable the device to be washable and waterproof. As shown in Figure 4c and Supporting Movie S4, water cannot permeate the SSCPS and slides down along the outer surface of the SSCPS. The charging curves of the SSCPS before and after being washed with water nearly have the same gradient (charging rate:  $\sim 178$  mV/min), indicating its reliability in operation. By pressing the SSCPS with hand at  $\sim 1.3$  Hz for a total time of about 8 min, the SSCPS can drive a wearable electronic watch for about 16 s (Figure 4e and Supporting Movie S5). It can be seen that the SSCPS can serve as a direct power source for wearable electronics by converting human motion into electricity.

## CONCLUSION

In summary, a type of stretchable and fully enclosed self-charging power system was developed and investigated, which seamlessly integrates a stretchable TENG that harvests energy and stretchable SCs that store the harnessed energy. The whole device was made of soft materials so that it can endure and extract energy from any kind of deformation. The fully enclosed structure and the hydrophobic property of the outer surface enabled the power system to be washable and waterproof. The power system was mounted on the human body to extract energy from diverse human motions, and it was able to drive an electronic watch. The TENG component, the SC component, and the integrated power system all have highly scalable fabrication processes. This work represents a promising route

to develop stretchable and wearable energy harvesters and power sources for stretchable and wearable electronics.

## EXPERIMENTAL SECTION

### Fabrication of the Stretchable Electrode (the CB Electrode).

1. Mix the base and curing agent of the silicone rubber (Ecoflex 00-30) (1:1, volume ratio) in a beaker. 2. Blend carbon black with the liquid silicone rubber (1:12, weight ratio). 3. Smear the composite over a piece of acrylic plate. Note that the acrylic plate was preprocessed with a release agent. 4. Cure the composite at a temperature of 30 °C for 5 h. 5. Peel the cured soft composite layer off the acrylic plate, which is a conductor. Note that the thickness of the stretchable electrode can be controlled by attaching layers of tape on the edge of the acrylic plate.

**Fabrication of the Stretchable Supercapacitor.** 1. Cut two pieces of the CB electrode to the same size. 2. Coat a composite of soluble polypyrrole and carbon black (4:1) on the surface of the CB electrode. 3. Prepare the PVA/H<sub>3</sub>PO<sub>4</sub> gel electrolyte: (1) add first 5 g of H<sub>3</sub>PO<sub>4</sub> and then 5 g of PVA powder into 50 mL of deionized water; (2) heat the mixture to 85 °C and stir the solution until it becomes clear. 4. Immerse the electrodes obtained from step 2 into the PVA/H<sub>3</sub>PO<sub>4</sub> solution for 10 min, with the two ends of the electrodes kept above the solution. 5. Take the electrodes out of the PVA/H<sub>3</sub>PO<sub>4</sub> solution and sandwich the two face-to-face electrodes with a wrinkled layer of polyethylene. Note that the wrinkled polyethylene was pretreated with the PVA/H<sub>3</sub>PO<sub>4</sub> solution. 6. The two ends of the electrodes serve as the electrode terminal. 7. Package the sandwiched electrodes with a silicon rubber wrapper.

**Fabrication of the Stretchable Power System.** The fabrication process is schematically depicted in Figure S2. 1. Pour the liquid silicone rubber into a mold. Note that two stretchable CB electrodes were prefabricated onto the mold. 2. Cure the silicone rubber at 30 °C for 5 h. 3. Peel off the cured rubber from the mold to get the triboelectric nanogenerator part. 4. Pour the liquid silicone rubber into a mold. 5. Put two serially connected SCs and the rectifier onto the silicone rubber when it becomes sticky. 6. Put the TENG part into the mold, fixing the TENG part by using a holder. 7. Fill the mold with liquid silicone rubber. 8. Cure the silicone rubber at room temperature for at least 24 h. All the parts must be kept still during the curing process. 9. Take the cured device out of the mold. Note that the liquid silicone rubber should be degassed before being poured into the molds.

**Experimental Arrangements.** 1. Influence of the distance between the contact object and the device on the performance: (1) fix the device in the moving direction of a linear motor; (2) attach an acrylic plate on the linear motor and set the distance between the acrylic plate and the device; (3) the periodic movement of the linear motor leads to the contact/separation of the device and the acrylic plate. 2. Influence of the stretching on the performance: (1) fix one end of the device; (2) attach the other end of the device onto a linear motor, which will periodically stretch the device. 3. Relationship between the current and frequency: a shaker (Labworks SC121) was applied to drive the contact/separation between the device and an acrylic plate.

**Measurement.** The surface morphologies of the silicone rubber, the stretchable CB electrode, and the SC's stretchable electrode were characterized by a Hitachi SU8010 field emission scanning electron microscope. The capacitance properties of the supercapacitor were tested by a potentiostat (Princeton Application Research) using EIS, CV, and GCD techniques. For the electrical output measurements of the triboelectric nanogenerator part, a programmable electrometer (Keithley model 6514) was utilized to test the open-circuit voltage and the charge, and a low noise current preamplifier (Stanford Research System model SR570) was adopted to test the short-circuit current.

## ASSOCIATED CONTENT

### Supporting Information

The Supporting Information is available free of charge on the ACS Publications website at DOI: 10.1021/acsnano.6b03007.

Figures S1–S5 (PDF)

Supporting Movie S1 (MP4)

Supporting Movie S2 (MP4)

Supporting Movie S3 (MP4)

Supporting Movie S4 (AVI)

Supporting Movie S5 (AVI)

## AUTHOR INFORMATION

### Corresponding Authors

\*E-mail: yuezhang@ustb.edu.cn.

\*E-mail: zlwang@gatech.edu.

### Author Contributions

<sup>#</sup>F. Yi, J. Wang, and X. Wang contributed equally to this work.

### Notes

The authors declare no competing financial interest.

## ACKNOWLEDGMENTS

This work is supported by the National Science Foundation (DMR-1505319), the Hightower Chair Foundation, the “Thousands Talents” program (China) for pioneer researcher (Z.L.W.) and his innovation team, the National Natural Science Foundation of China (grant nos. 51432005, 5151101243, 51561145021, 21274115, 51527802, and 51232001), the National Major Research Program of China (no. 2013CB932602), the Program of Introducing Talents of Discipline to Universities (B14003), Beijing Municipal Science and Technology Commission, and the Fundamental Research Funds for Central Universities. F.Y. would like to express her sincere gratitude to the China Scholarship Council (CSC) for the scholarship to help her study in the United States. Patents have been filed based on the research results presented in this article.

## REFERENCES

- (1) Kim, D.-H.; Lu, N.; Ma, R.; Kim, Y.-S.; Kim, R.-H.; Wang, S.; Wu, J.; Won, S. M.; Tao, H.; Islam, A.; Yu, K. J.; Kim, T.-I.; Chowdhury, R.; Ying, M.; Xu, L.; Li, M.; Chung, H.-J.; Keum, H.; McCormick, M.; Liu, P.; et al. Epidermal Electronics. *Science* **2011**, *333*, 838–843.
- (2) Sun, J.-Y.; Zhao, X.; Illeperuma, W. R. K.; Chaudhuri, O.; Oh, K. H.; Mooney, D. J.; Vlassak, J. J.; Suo, Z. Highly Stretchable and Tough Hydrogels. *Nature* **2012**, *489*, 133–136.
- (3) Tee, B. C.-K.; Chortos, A.; Berndt, A.; Nguyen, A. K.; Tom, A.; McGuire, A.; Lin, Z. C.; Tien, K.; Bae, W.-G.; Wang, H.; Mei, P.; Chou, H.-H.; Cui, B.; Deisseroth, K.; Ng, T. N.; Bao, Z. A Skin-Inspired Organic Digital Mechanoreceptor. *Science* **2015**, *350*, 313–316.
- (4) Park, S. I.; Brenner, D. S.; Shin, G.; Morgan, C. D.; Copits, B. A.; Chung, H. U.; Pullen, M. Y.; Noh, K. N.; Davidson, S.; Oh, S. J.; Yoon, J.; Jang, K.-I.; Samineni, V. K.; Norman, M.; Grajales-Reyes, J. G.; Vogt, S. K.; Sundaram, S. S.; Wilson, K. M.; Ha, J. S.; Xu, R.; et al. Soft, Stretchable, Fully Implantable Miniaturized Optoelectronic Systems for Wireless Optogenetics. *Nat. Biotechnol.* **2015**, *33*, 1280–1286.
- (5) Wang, C.; Hwang, D.; Yu, Z.; Takei, K.; Park, J.; Chen, T.; Ma, B.; Javey, A. User-Interactive Electronic Skin for Instantaneous Pressure Visualization. *Nat. Mater.* **2013**, *12*, 899–904.
- (6) Zhang, H.; Yang, Y.; Zhong, X.; Su, Y.; Zhou, Y.; Hu, C.; Wang, Z. L. Single-Electrode-Based Rotating Triboelectric Nanogenerator for Harvesting Energy from Tires. *ACS Nano* **2014**, *8*, 680–689.
- (7) Guo, H.; Leng, Q.; He, X.; Wang, M.; Chen, J.; Hu, C.; Xi, Y. A Triboelectric Generator Based on Checker-Like Interdigital Electrodes with a Sandwiched PET Thin Film for Harvesting Sliding Energy in All Directions. *Adv. Energy Mater.* **2015**, *5*, 1400790.
- (8) Yi, F.; Lin, L.; Niu, S.; Yang, J.; Wu, W.; Wang, S.; Liao, Q.; Zhang, Y.; Wang, Z. L. Self-Powered Trajectory, Velocity, and

Acceleration Tracking of a Moving Object/Body Using a Triboelectric Sensor. *Adv. Funct. Mater.* **2014**, *24*, 7488–7494.

(9) Lin, Z.-H.; Cheng, G.; Lee, S.; Pradel, K. C.; Wang, Z. L. Harvesting Water Drop Energy by a Sequential Contact-Electrification and Electrostatic-Induction Process. *Adv. Mater.* **2014**, *26*, 4690–4696.

(10) Yang, J.; Chen, J.; Su, Y.; Jing, Q.; Li, Z.; Yi, F.; Wen, X.; Wang, Z.; Wang, Z. L. Eardrum-Inspired Active Sensors for Self-Powered Cardiovascular System Characterization and Throat-Attached Anti-Interference Voice Recognition. *Adv. Mater.* **2015**, *27*, 1316–1326.

(11) Wang, Z. L.; Chen, J.; Lin, L. Progress in Triboelectric Nanogenerators As a New Energy Technology and Self-Powered Sensors. *Energy Environ. Sci.* **2015**, *8*, 2250–2282.

(12) Meng, B.; Tang, W.; Zhang, X.; Han, M.; Liu, W.; Zhang, H. Self-Powered Flexible Printed Circuit Board with Integrated Triboelectric Generator. *Nano Energy* **2013**, *2*, 1101–1106.

(13) Wang, S.; Lin, L.; Wang, Z. L. Nanoscale Triboelectric-Effect-Enabled Energy Conversion for Sustainably Powering Portable Electronics. *Nano Lett.* **2012**, *12*, 6339–6346.

(14) Zhang, X.-S.; Han, M.-D.; Wang, R.-X.; Zhu, F.-Y.; Li, Z.-H.; Wang, W.; Zhang, H.-X. Frequency-Multiplication High-Output Triboelectric Nanogenerator for Sustainably Powering Biomedical Microsystems. *Nano Lett.* **2013**, *13*, 1168–1172.

(15) Bae, J.; Lee, J.; Kim, S.; Ha, J.; Lee, B.-S.; Park, Y.; Choong, C.; Kim, J.-B.; Wang, Z. L.; Kim, H.-Y.; Park, J.-J.; Chung, U. I. Flutter-Driven Triboelectrification for Harvesting Wind Energy. *Nat. Commun.* **2014**, *5*, 4929.

(16) Zhu, G.; Chen, J.; Zhang, T.; Jing, Q.; Wang, Z. L. Radial-Arrayed Rotary Electrification for High Performance Triboelectric Generator. *Nat. Commun.* **2014**, *5*, 3426.

(17) Kim, K. N.; Chun, J.; Kim, J. W.; Lee, K. Y.; Park, J.-U.; Kim, S.-W.; Wang, Z. L.; Baik, J. M. Highly Stretchable 2D Fabrics for Wearable Triboelectric Nanogenerator under Harsh Environments. *ACS Nano* **2015**, *9*, 6394–6400.

(18) Yang, P.-K.; Lin, L.; Yi, F.; Li, X.; Pradel, K. C.; Zi, Y.; Wu, C.-I.; He, J.-H.; Zhang, Y.; Wang, Z. L. A Flexible, Stretchable and Shape-Adaptive Approach for Versatile Energy Conversion and Self-Powered Biomedical Monitoring. *Adv. Mater.* **2015**, *27*, 3817–3824.

(19) Zhang, Y.; Bai, W.; Cheng, X.; Ren, J.; Weng, W.; Chen, P.; Fang, X.; Zhang, Z.; Peng, H. Flexible and Stretchable Lithium-Ion Batteries and Supercapacitors Based on Electrically Conducting Carbon Nanotube Fiber Springs. *Angew. Chem., Int. Ed.* **2014**, *53*, 14564–14568.

(20) Meng, C.; Liu, C.; Chen, L.; Hu, C.; Fan, S. Highly Flexible and All-Solid-State Paperlike Polymer Supercapacitors. *Nano Lett.* **2010**, *10*, 4025–4031.

(21) Nystrom, G.; Marais, A.; Karabulut, E.; Wagberg, L.; Cui, Y.; Hamedi, M. M. Self-Assembled Three-Dimensional and Compressible Interdigitated Thin-Film Supercapacitors and Batteries. *Nat. Commun.* **2015**, *6*, 7259.

(22) Wang, S.; Lin, Z.-H.; Niu, S.; Lin, L.; Xie, Y.; Pradel, K. C.; Wang, Z. L. Motion Charged Battery as Sustainable Flexible-Power-Unit. *ACS Nano* **2013**, *7*, 11263–11271.

(23) Wang, J.; Wen, Z.; Zi, Y.; Zhou, P.; Lin, J.; Guo, H.; Xu, Y.; Wang, Z. L. All-Plastic-Materials Based Self-Charging Power System Composed of Triboelectric Nanogenerators and Supercapacitors. *Adv. Funct. Mater.* **2016**, *26*, 1070–1076.

(24) Pu, X.; Li, L.; Liu, M.; Jiang, C.; Du, C.; Zhao, Z.; Hu, W.; Wang, Z. L. Wearable Self-Charging Power Textile Based on Flexible Yarn Supercapacitors and Fabric Nanogenerators. *Adv. Mater.* **2016**, *28*, 98–105.

(25) Pu, X.; Li, L.; Song, H.; Du, C.; Zhao, Z.; Jiang, C.; Cao, G.; Hu, W.; Wang, Z. L. A Self-Charging Power Unit by Integration of a Textile Triboelectric Nanogenerator and a Flexible Lithium-Ion Battery for Wearable Electronics. *Adv. Mater.* **2015**, *27*, 2472–2478.

(26) Wang, J.; Li, X.; Zi, Y.; Wang, S.; Li, Z.; Zheng, L.; Yi, F.; Li, S.; Wang, Z. L. A Flexible Fiber-Based Supercapacitor-Triboelectric-Nanogenerator Power System for Wearable Electronics. *Adv. Mater.* **2015**, *27*, 4830–4836.

(27) Yi, F.; Lin, L.; Niu, S.; Yang, P. K.; Wang, Z.; Chen, J.; Zhou, Y.; Zi, Y.; Wang, J.; Liao, Q.; Zhang, Y.; Wang, Z. L. Stretchable-Rubber-Based Triboelectric Nanogenerator and Its Application As Self-Powered Body Motion Sensors. *Adv. Funct. Mater.* **2015**, *25*, 3688–3696.

(28) Chen, X.; Lin, H.; Chen, P.; Guan, G.; Deng, J.; Peng, H. Smart, Stretchable Supercapacitors. *Adv. Mater.* **2014**, *26*, 4444–4449.

(29) Niu, Z.; Dong, H.; Zhu, B.; Li, J.; Hng, H. H.; Zhou, W.; Chen, X.; Xie, S. Highly Stretchable, Integrated Supercapacitors Based on Single-Walled Carbon Nanotube Films with Continuous Reticulate Architecture. *Adv. Mater.* **2013**, *25*, 1058–1064.

(30) Chen, W.; Rakhi, R. B.; Hu, L.; Xie, X.; Cui, Y.; Alshareef, H. N. High-Performance Nanostructured Supercapacitors on a Sponge. *Nano Lett.* **2011**, *11*, 5165–5172.

(31) El-Kady, M. F.; Ihns, M.; Li, M.; Hwang, J. Y.; Mousavi, M. F.; Chaney, L.; Lech, A. T.; Kaner, R. B. Engineering Three-Dimensional Hybrid Supercapacitors and Microsupercapacitors for High-Performance Integrated Energy Storage. *Proc. Natl. Acad. Sci. U. S. A.* **2015**, *112*, 4233–4238.

(32) El-Kady, M. F.; Strong, V.; Dubin, S.; Kaner, R. B. Laser Scribing of High-Performance and Flexible Graphene-Based Electrochemical Capacitors. *Science* **2012**, *335*, 1326–1330.

(33) Zhu, Y.; Murali, S.; Stoller, M. D.; Ganesh, K. J.; Cai, W.; Ferreira, P. J.; Pirkle, A.; Wallace, R. M.; Cychosz, K. A.; Thommes, M.; Su, D.; Stach, E. A.; Ruoff, R. S. Carbon-Based Supercapacitors Produced by Activation of Graphene. *Science* **2011**, *332*, 1537–1541.

(34) Fan, F.-R.; Lin, L.; Zhu, G.; Wu, W.; Zhang, R.; Wang, Z. L. Transparent Triboelectric Nanogenerators and Self-Powered Pressure Sensors Based on Micropatterned Plastic Films. *Nano Lett.* **2012**, *12*, 3109–3114.

(35) Jeong, C. K.; Baek, K. M.; Niu, S.; Nam, T. W.; Hur, Y. H.; Park, D. Y.; Hwang, G.-T.; Byun, M.; Wang, Z. L.; Jung, Y. S.; Lee, K. J. Topographically-Designed Triboelectric Nanogenerator via Block Copolymer Self-Assembly. *Nano Lett.* **2014**, *14*, 7031–7038.